A KNUDSEN PUMP USING NANOPOROUS ZEOLITE FOR ATMOSPHERIC PRESSURE OPERATION

Naveen K. Gupta[*] *and Yogesh B. Gianchandani*
Department of Mechanical Engineering, University of Michigan, Ann Arbor, USA

ABSTRACT

This paper describes the use of naturally occurring nanoporous zeolite (clinoptilolite) for a miniature Knudsen pump. Based on the principle of thermal transpiration, these pumps have no moving parts, and are attractive for applications ranging from gas analyzers to cooling systems. The Knudsen pump requires flow channels that are in the free molecular or transitional flow regimes. Consequently, at atmospheric pressure, the pore diameters should be ≤100 nm, and large numbers of pores are necessary to permit meaningful flow. The initial prototype, operating at ≈50 K above room temperature, achieves a flow rate of ≈0.12 sccm with a small pressure load at the output, or a maximum pressure of ≈2.5 kPa when the flow is blocked. Its packaged volume is 55x55x12 mm^3.

1. INTRODUCTION

The past two decades have seen the miniaturization of various devices like gas sampling and testing systems, vacuum cavity pressure control systems, etc. [1-3]. These devices require pumps that are often disproportionately large. Some efforts to miniaturize the pumps based on the conventional operating principles have been reported, but reliability is often a challenge [4]. Designs that use peristaltic arrays of electrostatically driven diaphragms are promising. While extremely energy-efficient, they continue to evolve with respect to drive voltage requirements, and in reliability and complexity [5, 6]. Ultimately, there will likely have to be more than one solution. As a complement to the other approaches, the Knudsen pump, which is based on thermal transpiration, has some attractive features [7]. Conceived almost a century ago, it promises high reliability because there are no moving parts, eliminating one of the potential sources of failure.

For pump operation at or near atmospheric pressure, the flow channels must have hydraulic diameters of about 100 nm or less. The flow through these channels is in the free molecular flow regime or in the transitional regime between free molecular and viscous flow. The free molecular, transitional, and slip flow regimes are respectively represented by Kn >10, 0.1 < Kn <10, and 0.01 < Kn < 0.1. Here, Kn is the Knudsen number, defined as the ratio of the mean free path of the gas molecules to the characteristic length of the device [8].

With the recent advances in micromachining technology, the research community has been able to achieve flow channels with characteristic dimensions on the order of 100 nm. One such effort resulted in a fully micromachined Knudsen pump, reported by McNamara in 2005 [9]. This device achieved about 46.6 kPa. with 80 mW input power. Another device involved the use of synthetic aerogel, which is a porous material well-suited for gas flow by thermal transpiration. This device achieved a best-case pressure drop of 11.5 Torr (≈1.5 kPa) for helium [10]. While these efforts demonstrate experimental feasibility of miniature Knudsen pumps, there is room for improvement in performance, complexity, and cost.

This paper presents the use of a naturally-occurring nanoporous zeolite (clinoptilolite), which has been known for more than 250 years, in a miniature Knudsen pump. Providing an abundance of pores (> 2x10^{21} pores/cm^3) that are as small as 0.45 nm, it ensures the utility of the Knudsen pump at atmospheric pressure, while at the same time permitting substantial gas flow. The zeolite-based Knudsen pump discussed here provides at least 4 orders of magnitude more flow than our previous efforts [9, 11]. The following sections discuss underlying thermal transpiration theory, device design and fabrication, idealized simulations, experimental results, followed by a discussion that brings out some necessary details about the present effort.

2. THEORY

The phenomenon of thermal transpiration, on which the Knudsen pump is based, explains the difference in equilibrium pressures of two chambers that are maintained at different temperatures, while connected by a channel that permits gas flow in free molecular or transitional flow regime, but not in the viscous regime (Fig. 1) [12]. By equating the molecular flux between these chambers, it can be shown that the ratio of the pressures is related to the ratio of their absolute temperatures by:

$$\frac{P_2}{P_1} = \left(\frac{T_2}{T_1}\right)^{1/2} \quad (1)$$

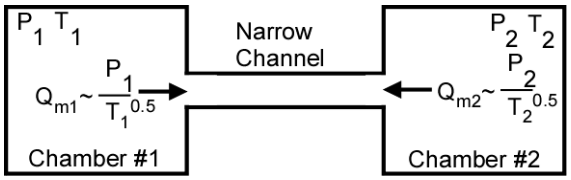

Fig. 1: Gas flux along the narrow channel connecting two chambers at different pressures and temperatures.

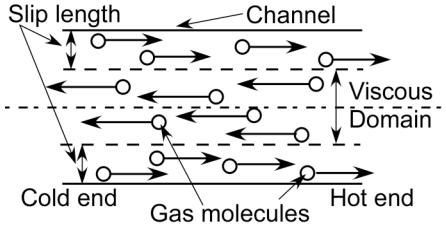

Fig. 2: Thermal transpiration at molecular level.

*Crspp. Auth.: gnaveen@umich.edu, 1301 Beal, Ann Arbor, MI-48109.

In the context of larger flow channels for which viscous flow is possible, thermal transpiration can also be explained as an equilibrium state attained by two opposing flow fields: thermal creep flow, which occurs close to the channel walls, and Poiseuille flow, designated by viscous flow in the central region of the channel (Fig. 2). By the virtue of the thermal creep flow, gas molecules move from the cold end to the hot end, whereas the Poiseuille flow is driven by the pressure gradient. For channels with hydraulic diameter on the order of the mean free path (or smaller), an observable pressure gradient can be observed across the channels because the Poiseuille flow, which acts to counterbalance the thermal creep flow otherwise, becomes vanishingly small.

Since the gas flow in thermal transpiration is not in the viscous flow regime, the models are based on the kinetic theory of gases. Most of the models used for the thermal transpiration are basically some manifestation of the Boltzmann equation (BE):

$$\frac{\partial f}{\partial t} + \bar{v}.\frac{\partial f}{\partial \bar{x}} + \bar{F}.\frac{\partial f}{\partial \bar{v}} = Q(f, f_*) \qquad (2)$$

where $\bar{F}$ is the imposed body force, $\bar{v}$ is the velocity vector, $\bar{x}$ is the position vector, f is the density function, $\partial f/\partial t$ is the change in molecular density, $\bar{v}.(\partial f/\partial \bar{x})$ represents molecules convected in/out of a region of space, $\bar{F}.(\partial f/\partial \bar{v})$ convection of molecules due to body force, $Q(f, f_*)$ represents the effect of intermolecular collisions, which necessarily needs to be simplified to solve BE analytically. One such thermal transpiration model, Sharipov's model, appears to be more suitable than others for micromachined channels [13]. It can be used to predict the mass flow rate along a narrow tube [14]:

$$\dot{M} = (Q_T \tau - Q_P \upsilon)\pi a^2 P\left(\frac{m}{2kT}\right)^{1/2} \qquad (3)$$

where T and P are the temperature and pressure along the channel respectively, m is mass of a gas molecule, k is the Boltzmann constant, a is the hydraulic radius of the narrow tube, Q_P and Q_T are the pressure and temperature coefficients that depend on rarefaction parameter δ given by

$$\delta = \frac{aP}{\mu}\left(\frac{m}{2kT}\right)^{1/2} \qquad (4)$$

where μ, τ, υ are viscosity, dimensionless temperature gradient and dimensionless pressure gradient respectively and are given by

$$\mu = \frac{1}{2}Nm\bar{u}\lambda; \upsilon = \frac{a}{P}\frac{dP}{dx}; \tau = \frac{a}{T}\frac{dT}{dx} \qquad (5a, b, c)$$

where N is the number of molecules per unit volume of gas, λ is the mean free path of gas molecules and $\bar{u}$ being the mean velocity of the gas molecules. Mean free path and mean velocity are given by:

$$\lambda = \frac{kT}{\sqrt{2}\pi D^2 P}; \bar{u} = \sqrt{\frac{8}{\pi}\frac{R_g T}{M}} \qquad (6a, b)$$

where k is the Boltzmann constant, D is the collision diameter of the gas molecule, R_g is the universal gas constant and M is the molecular mass of the gas.

3. Device Design and Fabrication

The device structure is designed to support a hot core and a cool exterior. The sectional view (Fig. 3) and 3D exploded view (Fig. 4) show the arrangement of various components (Fig. 5). The zeolite discs divide the device into three compartments. The central portion, with heating element sandwiched between the two zeolite discs, comprises the hot chamber, and has the gas outlet. Compartments formed between the zeolite discs and the PVC casings comprise the two cold chambers in the device. Each of these cold chambers has a provision for gas inlet. Embedded thermocouples provide the temperature of the hot and cold facets of the zeolite.

Zeolite is machined into 48 mm diameter and 2.3 mm thick discs and mechanically smoothed. Each of the zeolite discs has a thin sheet of perforated aluminum on both faces to facilitate a uniform in-plane temperature. The perforated aluminum discs chosen are 0.85 mm thick and have a porosity of 30% with pore diameter of 1.6 mm. The pore diameter of the aluminum sheet is chosen to ensure that the gas flow across the aluminum is in viscous domain. The two aluminum discs on the inner sides of the two zeolite discs sandwich a resistive heating element, which is a thin, flexible heating element consisting of an etched foil of 18.7

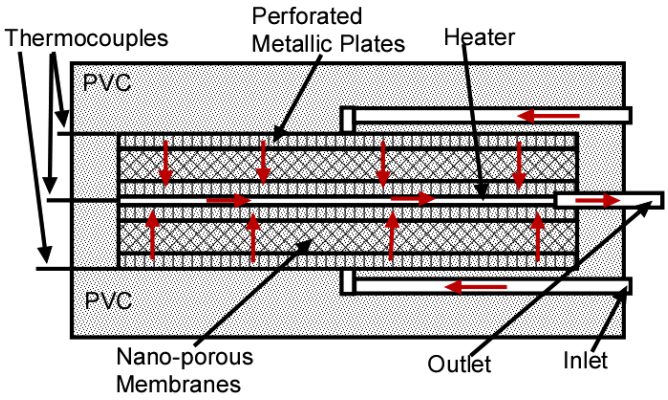

Fig. 3: Sectional view of the zeolite based Knudsen pump. The arrows show the direction of flow of the gas molecules within the device.

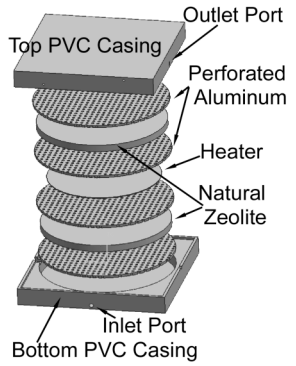

Fig. 4: Exploded view of the zeolite-based Knudsen pump.

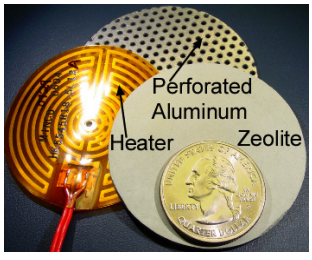

Fig. 5: Zeolite disc, thin, flexible heating element and perforated aluminum disc – used for the zeolite-based Knudsen pump (Fig. 4).

Ω laminated between layers of flexible insulation. This assembled structure is then encapsulated within an insulating casing, made of PVC in this case (Fig. 6). PVC, being a thermal insulator, supports the transverse temperature gradient across the thickness of the zeolite. A vacuum grade epoxy is used to bond inlet/outlet ports and thermocouples to the PVC structures and at other locations, as needed.

4. Simulations

Idealized Simulation Model

Figure 3 shows a sectional view of the Knudsen pump for which an idealized simulation model was developed. This model is termed as idealized because it assumes: (a) perfect zeolite structure, i.e., without any meso/macro pores [15], (b) perfect thermal contact at all interfaces, (c) uniform in-plane temperature, and (d) negligible gas flow resistance offered by all the elements, except the zeolite discs.

The hot and the cold facet temperatures of the zeolite disc, recorded experimentally, serve as an input to the Sharipov's model (Eqns. 3-6), which is used to evaluate the thermal transpiration effects induced by the zeolite disc subjected to this temperature gradient. Theoretically, the zeolite (clinoptilolite) has interconnected internal pores with pore diameter 0.45 nm and porosity of 34% (Fig. 7) [16].

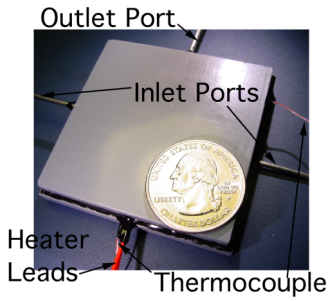

Fig. 6: Zeolite based Knudsen pump with PVC encapsulation. It has two inlet ports, an outlet port, leads for electrical connection to heater and two thermocouples to measure the hot and cold end temperatures.

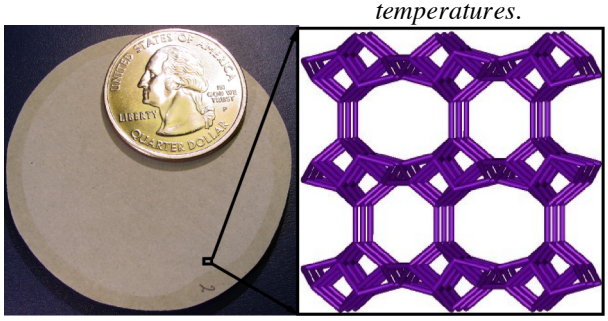

Fig. 7: Left: Zeolite disc – machined for the Knudsen pump; Right: Crystal structure of the Clinoptilolite with cell parameter – a = 1.75 nm, b = 1.76 nm and c = 0.74 nm. [Image on right is from the website of 'British Zeolite Assosiation'].

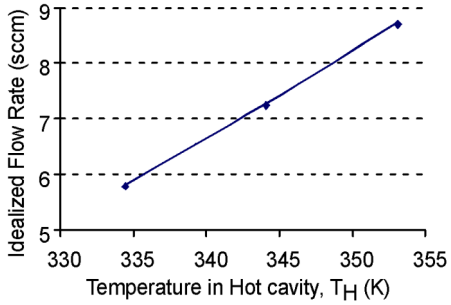

Fig. 8: Idealized flow rate, across the zeolite membrane, for which the experimentally observed temperatures are used as an input.

Results

Figure 8 shows the idealized gas flow rate obtained for various temperature boundary conditions derived from the experimentally measured temperature gradients. The experimentally observed temperature gradient, 14480 K/m across the 2.5 mm thick zeolite disc, is *ideally* expected to generate a gas flow rate 0.4 sccm/cm^2 – gas flow being measured at 1 atm and 300 K. The mass flow rate increases linearly with the temperature gradient, which, in turn, is limited primarily by the thermal conductivity of the zeolite. Simulations show that the insulating PVC casing can help to increase this temperature gradient for a given input power.

5. Experimental Results

The end facets of the device were placed against two heat sinks, thus keeping them near room temperature (Fig. 6). The system was designed for two different testing modes: 1) Pressure mode: a pressure sensor was attached to

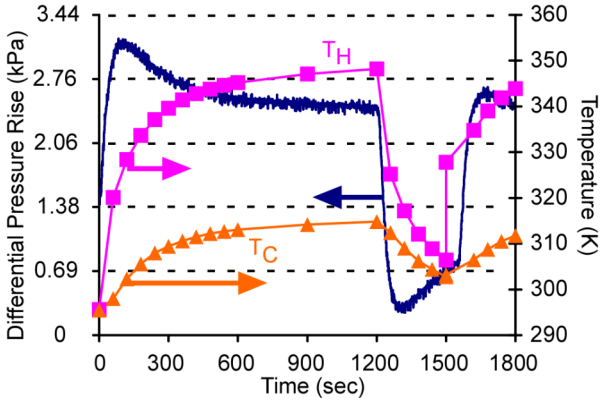

Fig. 9: Variation of the measured pressure at the sealed outlet of the Knudsen pump with the variation in the hot end temperature (T_H) and the cold end temperature (T_C).

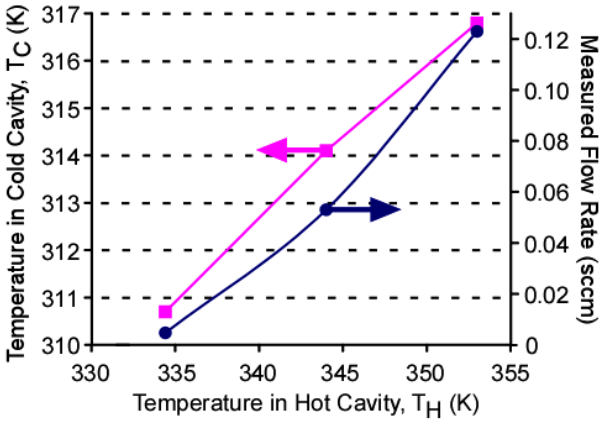

Fig. 10: Experimentally observed steady state flow rates for one side of the Knudsen pump, as the hot and cold cavity temperatures vary.

the sealed outlet of the Knudsen pump. 2) Flow rate: the outlet of the device was connected to a transparent tube (1.57 mm ø) with a small water droplet (≈2 mm long) in it and the velocity of the droplet was monitored for various input conditions. A piezoresistive pressure sensor (XTL-140, Kulite Semiconductor Products Inc., New Jersey) was used to measure the differential pressure built up in the sealed outlet, such that the reference was at the ambient pressure.

Only one side of the pump (i.e. only one of the two zeolite discs in the structure) was used for the preliminary characterization. The transient response of this device with sealed outlet (i.e. in the "pressure mode") is shown in Fig. 9. The device was able to generate a pressure of about 2.5 kPa with a heater temperature of 50 K above room temperature, while limiting the temperature rise on the cold side to 17 K. The device could successfully pump gas at 0.12 sccm, against a small load presented by the water droplet used to gauge the gas flow rate (Fig. 10).

6. Discussion and Conclusions

The idealized simulation results for the thermal transpiration flow across the zeolite disc deviate from the experimentally observed values significantly. With an input power of 5.35 W, a typical temperature drop of about 38 K (from 353 K to 317 K) was observed across the zeolite disc, which resulted in a gas flow rate of 0.12 sccm. However, the idealized simulation model suggests a gas flow rate of 8.7 sccm for the same temperature drop across the zeolite disc. There are a number of non-idealities that could be contributing to this mismatch, as discussed below.

Meso/Macro Pores in Natural Clinoptilolite

The presence of meso/macro pores at the crystal/grain boundaries as well as other defect such as cracks will result in a backflow of the gas being pumped across the zeolite disc. Literature suggests that the grain boundaries of natural clinoptilolite can have mesopores ranging from 25-50 nm upto 100 nm, and crystal boundaries have been reported to have macropores with an aggregate poresize of 500 nm [15]. Defects due to cracks are difficult to estimate at this stage of research, but it is notable that some defect may result from the choice of manufacturing technique.

Thermal Contact Resistance

Thermal contact resistance at various interfaces might result in undesirable temperature changes at these interfaces. Thus, the temperature reading observed experimentally from thermocouple could be significantly different from what actually exists across the nanoporous material. Lack of planarity of the zeolite-aluminum interface and surface asperities due to conventional machining processes may result in significant thermal contact resistance.

Composition of Clinoptilolite

Naturally occurring zeolites tend to have other zeolites and dirt included in their matrix as impurities. A very precise analysis might need to account for spatial variation in the thermal conduction and gas flow pathways.

In summary, we note that the reported zeolite-based single stage Knudsen pump, with a footprint of 55x55 mm^2, can generate a flow rate of 0.12 sccm for a temperature rise of 50 K, while restraining the temperature rise on cold facet to 17 K. This device can potentially operate at voltages as low as 1 V. The device has also been shown to be able to generate a pressure difference of 2.5 kPa across the zeolite, which can potentially be increased further by stacking multiple stages of this pump. Analysis suggests that further optimization of the parasitic losses from the device and with a suitable choice of zeolite material, the performance metric of the device can be improved significantly.

References

[1] S. Terry et al., "A gas chromatographic air analyzer fabricated on a silicon wafer," *IEEE Trans. Elec. Dev.*, 26, 1979, pp. 1880-86.

[2] E. T. Zellers et al., "A versatile MEMS gas chromatograph for determination of environmental vapor mixture," *Hilton Head,* 2004, pp. 61-66.

[3] H. Kim et al., "Micropump-driven high-speed MEMS gas chromatography system," *IEEE Transducers*, 2007, pp. 1505-08.

[4] N. T. Nguyen et al., "MEMS-micropumps: A review," *ASME J. Fluid Eng.*, 124(22), 2002, pp. 384-392.

[5] C. Cabuz et al., "The dual diaphragm pump," *IEEE MEMS*, 2001, pp. 519-22.

[6] H. Kim et al., "A fully integrates high-efficiency peristaltic 18-stage gas micropump with active microvalves," *IEEE MEMS*, 2007, pp. 127-30.

[7] M. Knudsen, "Eine revision der gleichgewichtsbedingung der gase. Thermische Molecularstr'omung," *Ann. Phys.*, Leipzig, 31, 1910, pp. 205-229.

[8] G. E. Karniadakis et al., *Microflows and Nanoflows: Fundamentals and Simulation*, Springer, New York, 2005, Ch. 1.

[9] S. McNamara et al., "On-chip vacuum generated by a micromachined Knudsen pump," *JMEMS,* 14(4), 2005, pp. 741-746.

[10] S. E. Vargo et al., "Initial results from the first MEMS fabricated thermal transpiration driven vacuum pump," *Rarefied Gas Dynamics: 22nd Int. Symp.*, 2001, pp. 502-09.

[11] N. K. Gupta et al., "Modeling and simulation of a surface micromachined Knudsen pump," *ASME-IMECE,* 2006, pp. 1-7.

[12] L. B. Loeb, *The Kinetic Theory of Gases*, McGraw Hill, 1934, pp. 355-359.

[13] N. K. Gupta et al., "Gas flow in nano-channels: thermal transpiration models with application to a Si-micromachined Knudsen pump," *IEEE Transducers*, 2007, pp. 2329-32.

[14] F. Sharipov, "Rarefied gas flow through a long tube at arbitrary pressure and temperature drop," *J. Vac. Sci. A,* 15(4), 1997, pp. 2434-36.

[15] P. Kowalczyk et al., "Porous structure of natural and modified clinptilolites," *J. Coll. Interf. Sc., 297, 2006, pp. 77-85.*

[16] F. Li et al., "Surface effect of natural zeolite (clinoptilolite) on the photocatalytic activity of TiO_2," *Applied Surface Science*, 252(5), 2005, p 1410-16.